

# Crack propagation in a glass particle-filled epoxy resin

## Part 1 *Effect of particle volume fraction and size*

J. SPANOUDAKIS, R. J. YOUNG

*Department of Materials, Queen Mary College, Mile End Road, London E1 4NS, UK*

Crack propagation in an epoxy resin reinforced with spherical glass particles has been followed using a double-torsion test. In particular the effect of strain rate, volume fraction and particle size upon the stability of propagation, the Young's modulus, the critical stress intensity factor,  $K_{Ic}$  and the fracture energy,  $G_{Ic}$  has been studied. It has been shown that the crack propagation behaviour can be explained principally in terms of crack pinning, although it has been found that propagation is also affected by blunting the breakdown of the particle-matrix interface. It has been demonstrated that crack-front pinning is consistent with a critical crack opening displacement criterion.

### 1. Introduction

The addition of rigid particles to epoxy resins can result in a significant improvement in the properties of the resin and a considerable reduction in cost. There is invariably an increase in the stiffness of the resin but the effect of the particles upon the fracture behaviour is complex. This paper is concerned with crack propagation in a model system consisting of different volume fractions of spherical glass particles with a narrow range of sizes reinforcing a well-characterized epoxy resin.

The fracture behaviour of multiphase polymers has been reviewed by several authors [1, 2] and there has been considerable interest over the years in crack propagation in brittle materials reinforced with rigid filler particles [3-13]. It is generally found that both the critical stress intensity factor,  $K_{Ic}$  and the fracture energy,  $G_{Ic}$  increase with the addition of rigid particles, at least for low volume fractions of filler. The most generally accepted explanation of this behaviour was proposed originally by Lange [3]. He suggested, using the analogy of a dislocation moving through a crystal, that a crack in a body possesses "line tension" and that when it meets an array of impenetrable obstacles it becomes pinned. In order to move past the obstacles he envisaged that the crack would have to bow out and showed that this would lead

to an increase in fracture energy. Lange [3] derived an equation relating the fracture energy,  $G_{Ic}$  of a composite to the separation of the obstacles,  $D_s$  of the form

$$G_{Ic} = G_{Ico} + \frac{T_L}{D_s} \quad (1)$$

where  $T_L$  is the "line tension" of the crack and  $G_{Ico}$  is the fracture energy of the matrix. The interparticle separation is a function of both the particle diameter  $d_p$  and the volume fraction of particles  $V_p$  and is given [9] by

$$D_s = \frac{2d_p(1 - V_p)}{3V_p} \quad (2)$$

Combining Equations 1 and 2 produces an equation which predicts that for a given particle size,  $d_p$ , the fracture energy should increase with increasing  $V_p$ . This is precisely what is found for low volume fractions of filler [7-9] but  $G_{Ic}$  is normally found to reach a maximum at a particular value of  $V_p$  and then fall with the further addition of particles, implying that there may be another mechanism which competes with crack-front pinning at high volume fractions of filler. Another problem that arises with the Lange theory (Equation 1) is that when  $G_{Ic}$  is plotted against  $1/D_s$  for different sizes of filler particles in brittle

polymers, lines of different initial slope are obtained [7, 9]. This clearly implies that the line tension,  $T_L$  is a function of particle size. Lange [14] found a similar problem with the glass/ $Al_2O_3$  system and introduced a dimensionless parameter  $F(d)$  into Equation 1

$$G_{Ic} = G_{Ic0} + \frac{F(d)T_L}{D_s} \quad (3)$$

where  $0 \leq F(d) \leq 1$ . However, this modification is not very satisfactory and the physical meaning of  $F(p)$  is unclear. The problem was resolved by Evans [4] who carried out a detailed calculation of  $T_L$  and demonstrated that the line energy contribution to the fracture energy depended upon both the particle size and spacing. More recently Green *et al.* [11, 12] have extended the analysis of Evans [4]. They have examined, both experimentally and theoretically, the effects of particle shape and particle/matrix adhesion upon fracture in model brittle composites of nickel spheres in a glass matrix.

In this present work crack propagation in a model system consisting of five different volume fractions of five different sized spherical glass particles in an epoxy resin matrix is studied. The way in which the critical values of stress intensity factor,  $K_{Ic}$  and fracture energy,  $G_{Ic}$  vary with testing conditions and the size and volume fraction of particles are determined. The extent to which the data can be explained by the various theories of particle reinforcement is then discussed.

## 2. Experimental details

### 2.1. Materials

The materials used in this present study were an epoxy resin (Epikote 828) hardened with tetraethylene pentamine (TEPA) which is a mixed primary and secondary amine, and spherical glass particles (Ballotini). This particular resin/hardener system was chosen because crack propagation takes place in a stable manner in the unfilled state. The glass particles were obtained in a variety of different size ranges and so they were sieved into sharp fractions of average particle diameters of 4.5, 16, 32, 47 and 62  $\mu m$ . The distribution of particle size was determined by examining several hundred particles of each size fraction in a scanning electron microscope. They were given no special surface pretreatment but were cleaned with isopropanol and dried at 100°C *in vacuo* before moulding to remove any contaminants.

### 2.2. Moulding and characterization

The epoxy resin was degassed for 1 h at 80–90°C and a measured quantity of particles were added. The mixture was gently stirred at this temperature for a further period of time to allow air bubbles generated during mixing to escape. The temperature was allowed to drop to 60°C when the TEPA (10% of the weight of the resin) was added. The mixture then was stirred carefully for a few minutes and poured into the mould. This consisted of two square glass plates held together by PTFE spacers 3.9 mm apart and covered with polyurethane release agent. The mixture was allowed to harden for 24 h at room temperature and was then post-cured at 80°C for 8 h.

The mouldings were carefully characterized to ensure that the volume fractions of particles and void content were known accurately. The densities of samples from each moulding were determined by weighing in air and water. Samples were also ashed to determine the mass of resin and glass. Since the specific gravities of the resin (1.17) and the glass are known (2.46) the volume fraction of particles and voids could be determined. The volume of voids was found to be always less than 2% and so the volume fractions of particles were thought to be close to their nominal values of 0.10, 0.18, 0.30, 0.40 and 0.46.

Another problem that can be encountered with these composites is local variation in particle volume fraction due to settlement or aggregation. This was checked by examining polished sections in an optical microscope and the distributions were found to be uniform. Fig. 1 shows a section from a typical moulding containing 30% of particles by volume examined in reflected light. It can be seen that there is a good distribution of

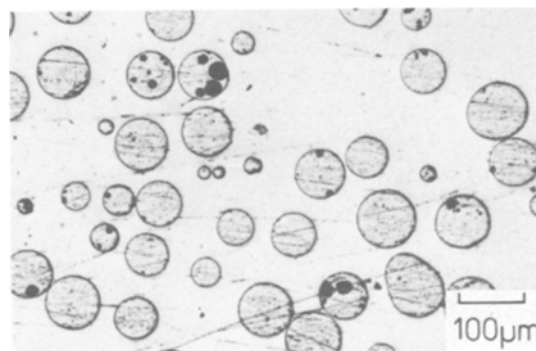


Figure 1 Optical micrograph of a polished section of a moulding containing 62  $\mu m$  diameter particles ( $V_p = 0.30$ ).

particles and no aggregation or settlement in this moulding.

### 2.3. Crack propagation measurements

Crack propagation in the various composites was investigated using the double torsion (DT) test which gave good control of the growing crack and enabled easy and rapid determination of the critical stress intensity factor,  $K_{Ic}$ . The technique has been described in detail elsewhere [1, 8] and it can be shown that  $K_{Ic}$  is independent of crack length and for an elastic material given approximately by

$$K_{Ic} = P_c W_m \left[ \frac{3(1 + \nu)}{W t^3 t_n} \right]^{1/2} \quad (4)$$

where  $P_c$  is the critical load,  $W_m$  the moment arm,  $\nu$  the Poissons ratio of the material,  $W$  the specimen width,  $t$  the plate thickness and  $t_n$  the plate thickness in the plane of the crack.

The 3.9 mm thick moulded composite sheets were cut into rectangular plates 60 mm long and 30 mm wide. They were notched at one end and a V-shaped groove, 1.2 mm deep, was machined along the centre of one face.

The specimens were then deformed in the DT rig [1, 8] in an Instron Universal testing machine at room temperature ( $22 \pm 2^\circ \text{C}$ ) using a two decade range of crosshead speeds, from  $0.05$  to  $5 \text{ mm min}^{-1}$ . The value of  $K_{Ic}$  was determined from Equation 4 using the measured value of  $P_c$  and knowing the specimen dimensions. No attempt was made to measure the crack velocity.

### 2.4. Young's modulus and fracture energy

The Young's modulus of each type of composite was determined in flexure so that the fracture energy,  $G_{Ic}$  could be obtained from  $K_{Ic}$  through the relationship [1]

$$G_{Ic} \sim K_{Ic}^2/E \quad (5)$$

where  $E$  is the Young's modulus. Fractured halves of the DT specimens were used in a three-point bend rig and the value of  $E$  was determined from the variation of load with displacement and the specimen dimensions [8]. The tests were again carried out at room temperature using crosshead speeds ranging from  $0.05$  to  $5 \text{ mm min}^{-1}$ . The fracture energy was determined through Equation 5 using the same crosshead speed for both  $K_{Ic}$  and  $E$ . Obviously, because of the difference in specimen geometry it would be better to use the same

strain rate. However, this is difficult to define for both the DT and three-point bend test.

### 2.5. Fractography

The fracture surfaces of a large number of specimens were examined in a scanning electron microscope, Jeol JXA-50A, operated at  $15 \text{ kV}$ . Before observation the specimens were sputter-coated with a thin layer, ( $\sim 20 \text{ nm}$ ) of gold to make the surfaces conductive and reduce charging.

## 3. Results and discussion

### 3.1. Stability of crack propagation

It was found that in the composites cracks tended to propagate in a continuous stable manner for certain compositions and for other compositions propagation was found to be of the unstable stick/slip type. This behaviour has been widely reported for similar composites [6, 7, 13] and for unfilled thermosetting polymer matrices [15–17]. The type of crack propagation has a significant affect upon the load/displacement curves as shown in Fig. 2. When unstable propagation occurs the load/displacement curve has a characteristic saw-tooth shape (Fig. 2a). The values of  $P_i$  and  $P_a$  correspond to loads at crack initiation and arrest. The initiation and arrest values of  $K_{Ic}$  and  $G_{Ic}$  can be determined from  $P_i$  and  $P_a$  through Equations 4 and 5. In contrast, when stable propagation occurs the crack propagates at a constant load (Fig. 2b). This corresponds to single values of  $K_{Ic}$  and  $G_{Ic}$ . It should be pointed out that the unstable stick/slip propagation occurs from some compositions even though propagation in the matrix is always continuous. This is a clear indication that the presence of the glass particles can cause propagation to become unstable. It will be shown later that the unstable stick/slip propagation is probably due to crack-tip blunting as in the case of unfilled thermosetting polymers [16, 17].

### 3.2. Stress intensity factor

#### 3.2.1. Effect of crosshead speed

One of the most interesting aspects of this investigation is the observation that crosshead speed has a significant effect upon the stability of crack propagation. This behaviour is well-known for unfilled epoxy resins [15–17] but it has not previously been reported in particle-filled composites. The effect of crosshead speed can be clearly seen in Figs. 3 and 4 for two different average particle sizes,  $4.5$  and  $62 \mu\text{m}$ . In both

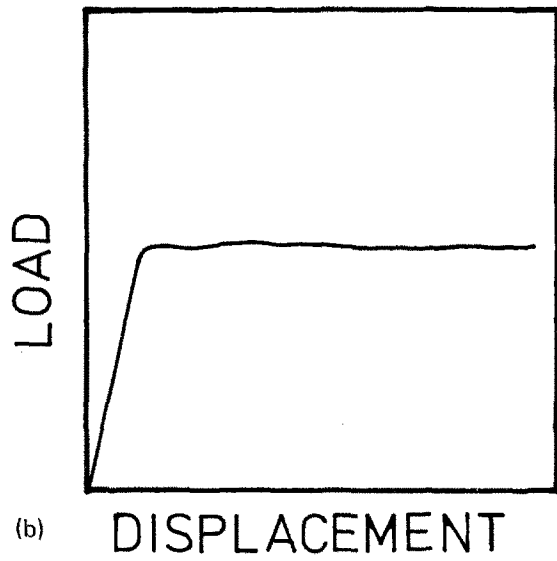
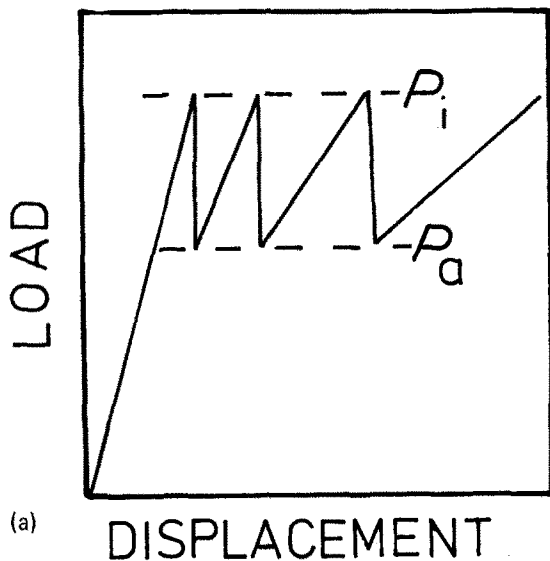


Figure 2 Typical schematic load/displacement curves for the particle-filled epoxy resin. (a) Continuous, stable propagation. (b) Unstable, stick/slip propagation.

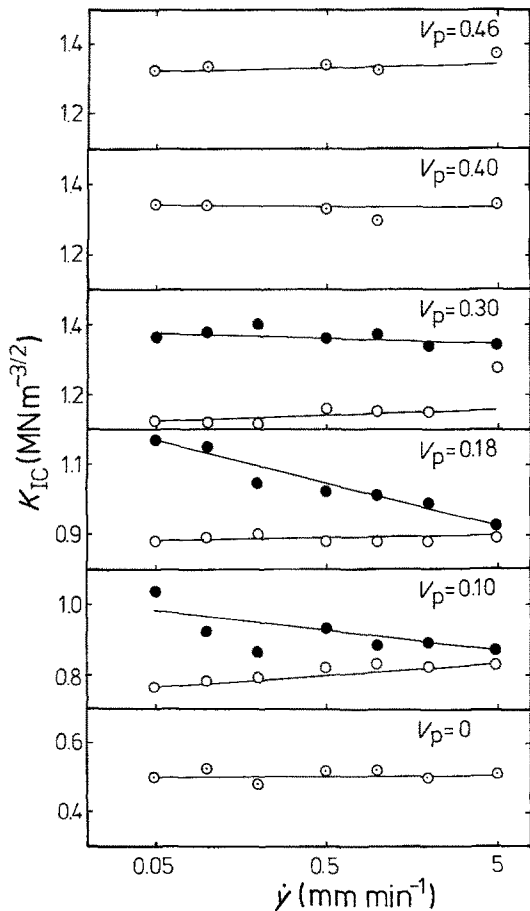


Figure 3 Variation of  $K_{Ic}$  with crosshead speed,  $\dot{y}$ , for different volume fractions of  $4.5\ \mu\text{m}$  diameter particles. ● – crack initiation, ○ – crack arrest, and ⊙ – continuous propagation.

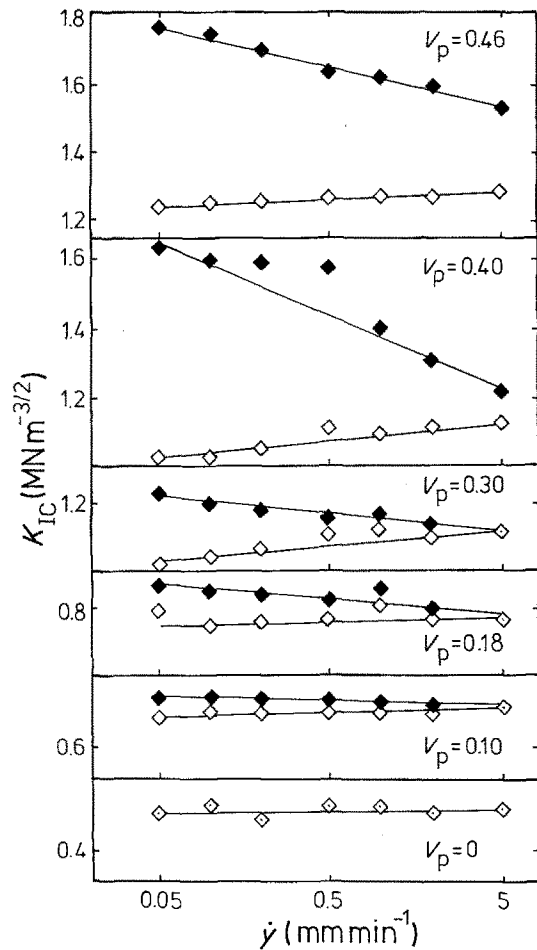


Figure 4 Variation of  $K_{Ic}$  with crosshead speed,  $\dot{y}$ , for different volume fractions of  $62\ \mu\text{m}$  diameter particles. ◆ – crack initiation, ◇ – crack arrest, and ◆ – continuous propagation.

cases it can be seen that the value of  $K_{Ic}$  for crack initiation decreases with increasing crosshead speed, whereas the arrest value remains constant or even increases slightly. This means that the cracks tend to propagate in a more stable manner as the crosshead speed is increased.

This behaviour is very similar to the unfilled epoxy resins where virtually identical transitions in behaviour have been reported on increasing the crosshead speed, or reducing the test temperature [15]. This behaviour in epoxy resins has been explained successfully in terms of crack blunting [16, 17]. It has been shown that the variation of the yield stress of the unfilled resin with testing-conditions will lead to cracks becoming blunted at low crosshead speeds and high temperatures, giving rise to unstable crack propagation. Although the yield stresses of the particle-filled composites have not been measured it would seem likely that they will increase with crosshead speed and so a similar blunting mechanism may apply. This is discussed further in Section 4.3.

### 3.2.2. Effect of particle volume fraction

It can be seen from the plots in Figs. 3 and 4 that the volume fraction of particles,  $V_p$  has a significant effect upon  $K_{Ic}$ , and the stability of crack propagation for the composites for both the 4.5 and 62  $\mu\text{m}$  particles. The values of  $K_{Ic}$  for initiation and arrest both increase with an increasing particle volume fraction and propagation tends to become unstable. However, at high volume fractions propagation becomes stable again for the 4.5  $\mu\text{m}$  particles. In contrast for the resin containing the larger 62  $\mu\text{m}$  particles there is no tendency for propagation to stabilize at high volume fractions.

The effect of  $V_p$  upon  $K_{Ic}$  can be seen more clearly in Fig. 5 where  $K_{Ic}$  is plotted directly against  $V_p$  for a fixed crosshead speed ( $0.5 \text{ mm min}^{-1}$ ). For each particle size both the initiation and propagation values of  $K_{Ic}$  tend to increase with increasing  $V_p$ . For the smaller particles propagation tends to stabilize at high volume fractions and when this happens  $K_{Ic}$  reaches a plateau level. In the case of the larger, 47  $\mu\text{m}$  particles propagation is always unstable and  $K_{Ic}$  is still increasing when  $V_p = 0.46$ .

Most previous investigations have tended to concentrate upon the effect of  $V_p$  upon the fracture energy,  $G_{Ic}$  [6, 7, 9, 10, 13]. This has, to a certain extent, tended to make the analysis of the behaviour more complicated than necessary

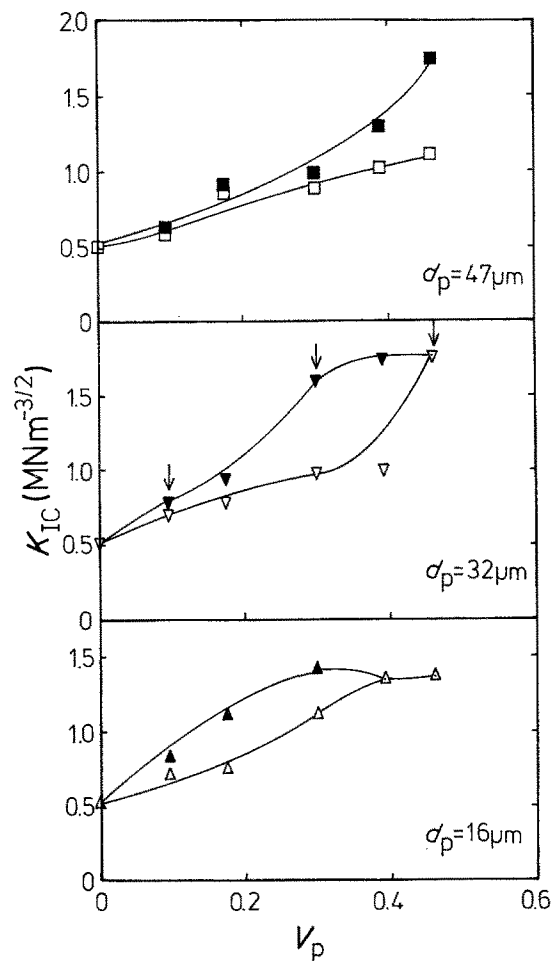


Figure 5 Variation of  $K_{Ic}$  with  $V_p$  for particles of different size. The closed points are for initiation and the open ones for arrest. (The arrows indicate the specimens which have their fracture surfaces shown in Fig. 12.)

since  $V_p$  also has a strong effect upon the Young's modulus of the composites. The effect of particle volume fraction is discussed in more detail later in Section 4 where it will be shown that the relationship between  $K_{Ic}$  and  $V_p$  can be interpreted in terms of the crack pinning mechanisms.

### 3.2.3. Effect of particle size

Unlike the particle volume fraction,  $V_p$ , the particle size only has a secondary effect upon  $K_{Ic}$ . Fig. 6 shows the variation of  $K_{Ic}$  with particle diameter,  $d_p$ , for three different volume fractions. It can be seen that for the lowest value of  $V_p$ , 0.10,  $K_{Ic}$  decreases with increasing particle size. In contrast, for  $V_p = 0.30$ ,  $K_{Ic}$  peaks at a particle diameter of 32  $\mu\text{m}$ . The picture is further complicated at high volume fractions where  $K_{Ic}$  increases

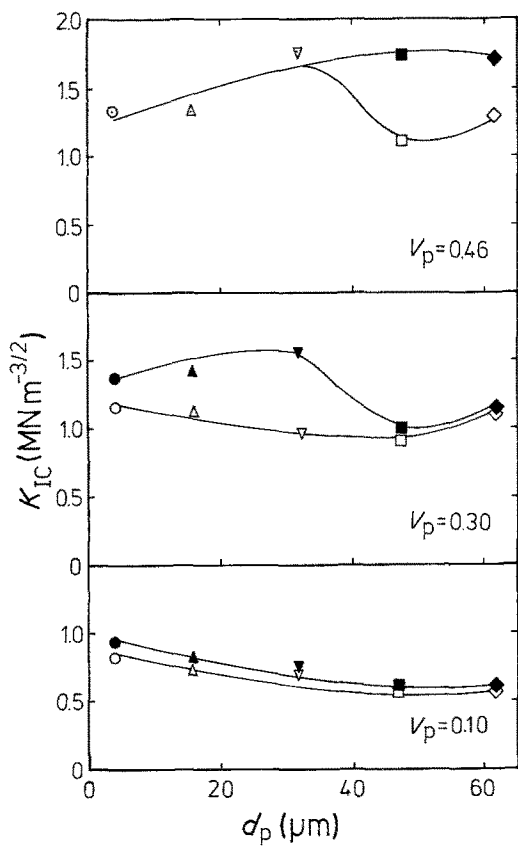


Figure 6 Variation of  $K_{IC}$  with  $d_p$  for different volume fractions of particles. The closed points are for initiation and the open ones for arrest.

with increasing value of  $d_p$  and propagation becomes unstable at and above  $d_p = 47 \mu\text{m}$ .

It should be noted that the highest values of  $K_{IC}$  are found for the composites containing the highest volume fractions of the largest particles.

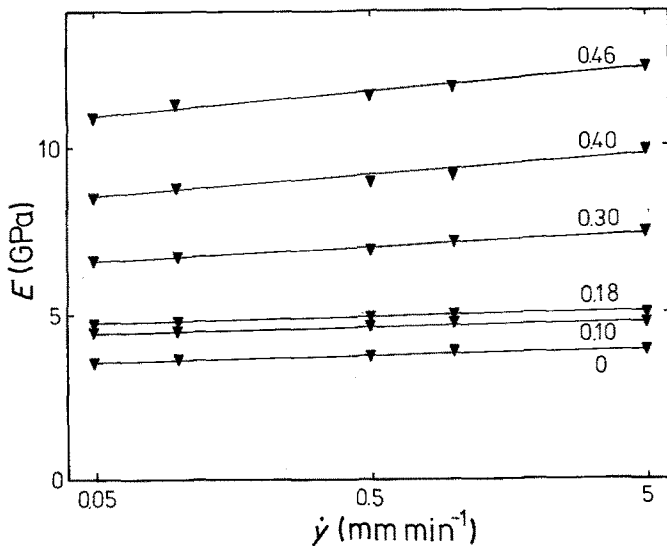


Figure 7 Variation of Young's modulus,  $E$ , with crosshead speed,  $\dot{\gamma}$ , for different volume fractions of particles ( $d_p = 32 \mu\text{m}$ ).

This has important implications for the design of strong composites

### 3.3. Young's modulus

Although this project was concerned principally with the mechanisms of crack propagation in particle-filled epoxy resins, it was necessary to measure the value of Young's modulus  $E$  for the composites in order to convert  $K_{IC}$  to  $G_{IC}$ . Because of this the opportunity has been taken to comment upon the factors which control the stiffness of the composites and to compare the data obtained with some of the many theories used to explain the stiffening polymers through particle reinforcement. These have been discussed in detail elsewhere [18].

#### 3.3.1. Effect of crosshead speed

Fig. 7 shows the variation of Young's modulus with crosshead speed for different volume fractions of  $32 \mu\text{m}$  particles. In each case the modulus increases with increasing crosshead speed. Since the strain-rate is proportional to the crosshead speed the increase in modulus can be thought of as the normal strain-rate dependent behaviour of a polymer. The slope of the lines in Fig. 7 increases as the volume fraction of particles increases. At first sight this may appear to be a result of the increase in modulus level with volume fraction. However, more careful examination shows that the strain-rate dependence of  $E$  is higher for the higher volume fraction formulations. For example, the modulus of the unfilled resin increases 9% over 2 decades of strain rate whereas the modulus

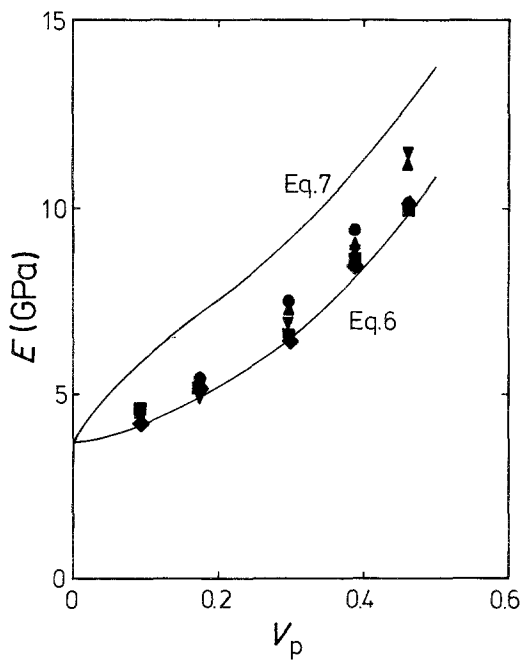


Figure 8 Variation of  $E$  with  $V_p$  for different particle diameters. The two lines correspond to Equations 6 and 7. ● -  $d_p = 4.5 \mu\text{m}$ , ▲ -  $d_p = 16 \mu\text{m}$ , ▼ -  $d_p = 32 \mu\text{m}$ , ■ -  $d_p = 47 \mu\text{m}$ , ◆ -  $d_p = 62 \mu\text{m}$ .

of the resin with  $V_p = 0.46$  increases by about 15% for the same strain rate increase. The effect has been found to be similar for other particle sizes. It is not clear why the composite with the highest volume fraction of particles should have the highest strain-rate dependence as glass is not a viscoelastic material. This would appear to be an area meriting further investigation.

### 3.3.2. Effect of particle volume fraction

There is a strong dependence of the modulus of the composites upon the volume fraction of particles,  $V_p$ , as shown in Fig. 8. This behaviour is well documented [8, 18, 19] and a variety of theories have been developed to explain the dependence of the modulus of the composite upon the particle volume fraction,  $V_p$ . The data can be fitted to several theories [18] but the two curves in Fig. 8 are the upper and lower bounds of the calculations of Ishai and Cohen [19]. They modelled the composite as cubic particles surrounded by a shell of matrix. If the boundary of the cube is subjected to a uniform displacement then

$$E_c = E_0 \left\{ 1 + \frac{V_p}{[m/(m-1) - V_p^{1/3}]} \right\} \quad (6)$$

where  $E_c$  and  $E_0$  are the composite and matrix moduli and  $m = E_p/E_0$ , the modular ratio, where  $E_p$  is the modulus of the particles. If the boundary of the cube is subjected to a uniform stress then it follows that

$$E_c = E_0 \left[ \frac{1 + (m-1)V_p^{2/3}}{1 + (m-1)(V_p^{2/3} - V_p)} \right] \quad (7)$$

Equations 6 and 7 have been plotted in Fig. 8 assuming that  $E_p = 73.1 \text{ GPa}$  [18] and taking  $E_0$  as the value measured when  $V_p = 0$  (3.71 GPa). It can be seen that the experimental data fall closer to the lower bound corresponding to the case of uniform displacement at the particle/matrix boundary.

### 3.3.3. Effect of particle size

The theories that are used to explain the variation of the modulus of polymer composites with volume fraction do not normally take into account the effect of particle size. However, it can be seen from Fig. 9 that there is a clear decrease in the modulus of a composite with increasing particle size for a given volume fraction of particles. This can also be seen in Fig. 8 where the composites containing the smallest particles tend to have the highest moduli.

The relatively low values of Young's modulus for large particle sizes has been attributed to

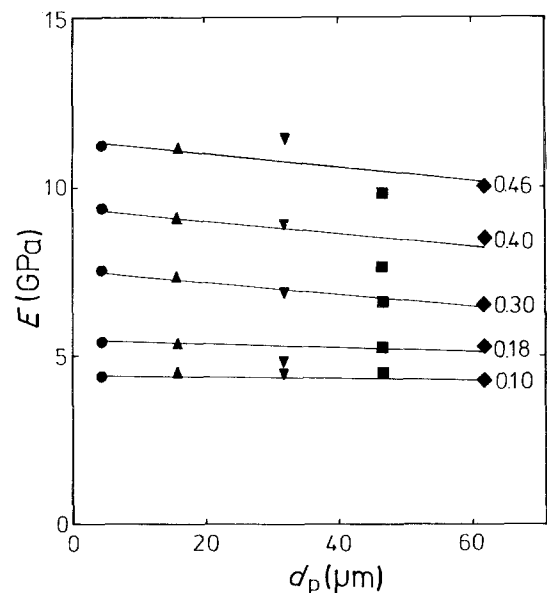


Figure 9 Dependence of  $E$  upon  $d_p$  for composites of different volume fraction. The symbols have the same meaning as in Fig. 8.

a “skin” effect [20]. Lewis and Nielsen [20] suggested that when moduli are determined in flexure, as in this present study, the properties of the surface are emphasized at the expense of the interior. This tends to be worse for large particles where the surface “skin” is depleted of particles. This could explain why the modulus has been observed in this present study to drop with increasing particle size and the error due to the “skin” effect can be removed by extrapolating to zero particle size.

### 3.4. Fracture energy

The fracture energy was determined using the Equation 5 with the values of  $K_{Ic}$  and  $E$  measured previously. It was found that  $E$  did not vary strongly with strain rate (Fig. 7) and so the variation of  $G_{Ic}$  with crosshead speed should be similar to that of  $K_{Ic}$  (Figs. 3 and 4). However,  $E$  was found to vary significantly with  $V_p$  (Fig. 8) and also to a certain extent with  $d_p$  (Fig. 9) and so only the variations of the fracture energy with particle volume fraction and size will be considered here.

#### 3.4.1. Effect of particle volume fraction

The value of  $K_{Ic}$  is found to increase and eventually reach a plateau value with an increasing volume fraction of particles (Fig. 5). However, the fracture energy behaves very differently as can be seen in Fig. 10. For the small sized particles ( $16\mu\text{m}$ ) the initiation value of fracture energy peaks at  $V_p \sim 0.17$ . As the particle size is increased to  $32\mu\text{m}$  the peak value of  $G_{Ic}$  is higher and occurs at a higher value of  $V_p$  ( $\sim 0.30$ ). For the larger particles ( $47\mu\text{m}$ )  $G_{Ic}$  increases monotonically with increasing  $V_p$  and does not peak. The arrest values of fracture energy tend to increase with  $V_p$  and propagation becomes continuous in the composites when the volume fraction of particles is considerably higher than the value of  $V_p$  which gives the maximum value of  $G_{Ic}$ .

The dependence of  $G_{Ic}$  upon  $V_p$  shown in Fig. 10 has been found by several groups of workers for similar systems [6, 7, 9, 10, 13]. However, the size of maximum value of  $G_{Ic}$  and its variation with  $V_p$  for different particle sizes was not explained satisfactorily in these earlier investigations. This is discussed in Section 4.6.

#### 3.4.2. Effect of particle size

It is found that for a given value of  $V_p$  the particle

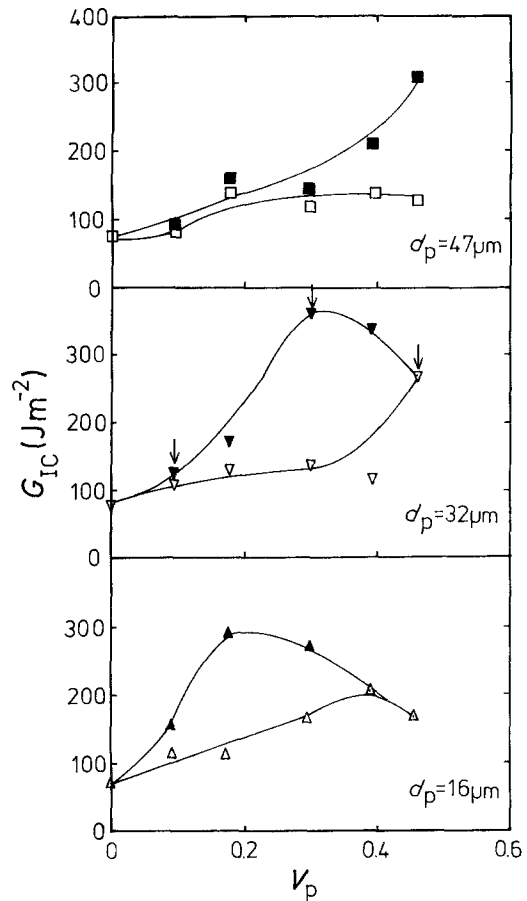


Figure 10 Variation of  $G_{Ic}$  with  $V_p$  for different particle diameters. The closed points are for crack initiation and the open ones for arrest. (Fracture surfaces of the compositions arrowed are shown in Fig. 12).

size has a significant effect upon both the value of fracture energy and the nature of crack propagation. For a low volume fraction ( $V_p = 0.010$ )  $G_{Ic}$  drops with increasing particle size to a minimum value when  $d_p \sim 47\mu\text{m}$ . For an intermediate volume fraction ( $V_p = 0.30$ ) the initiation value of  $G_{Ic}$  peaks at particle diameter of  $32\mu\text{m}$ . In the composites containing a high volume fraction of particles ( $V_p = 0.46$ ) propagation is continuous up to a diameter of  $32\mu\text{m}$  above which it becomes stick/slip. The value of  $G_{Ic}$  increases at first and then reaches a plateau level. It can be seen that curves in Fig. 11 are of a similar form to those in Fig. 6. This is because the dependence of modulus upon particle size (Fig. 9) is not particularly strong.

### 3.5. Fractography

The fracture surfaces of a large number of speci-



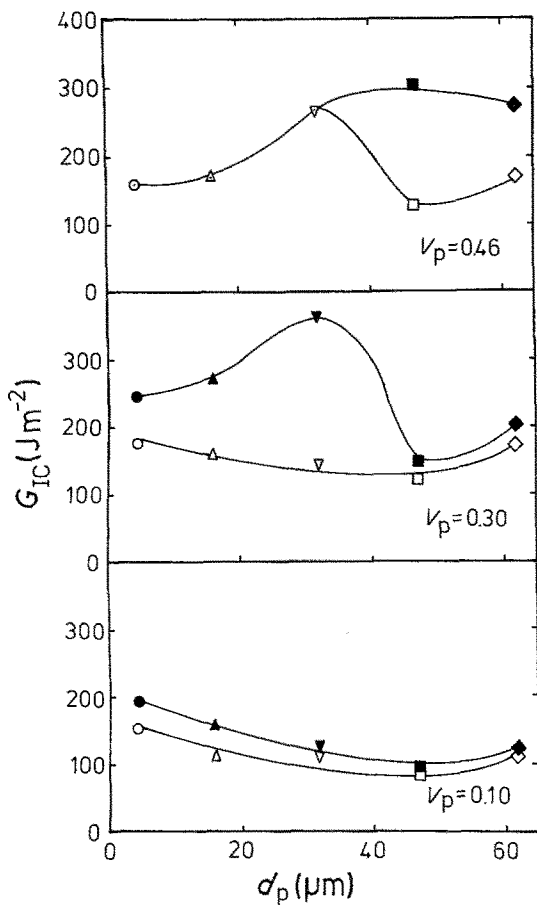


Figure 11 Variation of  $G_{IC}$  with  $d_p$  for different volume fractions of particles. The closed points are for crack initiation and the open ones are for arrest.

mens were examined but it is only possible to present a representative few micrographs here. In Fig. 12 scanning electron micrographs are given for three different volume fractions of  $32\ \mu\text{m}$  particles fractured at a crosshead speed of  $0.5\ \text{mm}\ \text{min}^{-1}$ . For the lowest volume fraction (Fig. 12a) it can be seen that the particles are widely spaced but that there are characteristic tails behind each particle pointing in the direction of crack propagation. When  $V_p = 0.30$  (Fig. 12b) the particles are much closer together but tails can still be seen behind each particle. In contrast, for the highest volume fraction (Fig. 12c) the particles are very close together and there is no evidence of any tails. The presence of tails behind the particles is often taken as an indication that pinning of the crack front has taken place. However, the absence of tails does not necessarily mean that no pinning occurs since at high volume fractions of particles there may be considerable overlap of the second-

ary cracks. The change in fracture surface appearance is discussed in more detail in Section 4.4.

#### 4. Mechanisms of particulate reinforcement

In the previous section the way in which the different testing and structural variables affect  $K_{IC}$  and  $G_{IC}$  have been discussed. It was found that both of these parameters increase with particle volume fraction at least at low values of  $V_p$  but that at higher volume fractions the behaviour can be more complex.

The various theories concerned with the mechanisms of particulate reinforcement in brittle materials have been reviewed briefly in the introduction. The most generally-accepted explanation of the increase of  $K_{IC}$  and  $G_{IC}$  with  $V_p$  is that it is due to crack-front pinning. In this section the early theory of Lange [3] is discussed, first of all, and the development due to Evans [4] and Green *et al.* [12] are described in detail.

##### 4.1. Crack pinning theory of Lange

This theory has been described in the Introduction (Section 1) and it predicts that there should be a linear increase in  $G_{IC}$  when it is plotted against  $1/D_s$ , the reciprocal of the interparticle separation, as given by Equation 1. It can be seen from Fig. 13 that the slope of such plots is linear at low volume fractions of particles but that some compositions show deviations from linearity and even maxima in  $G_{IC}$ . The initial slopes of the lines are also found to increase with particle volume fraction. The variation in slope has been explained by assuming that the line tension,  $T_L$  varies with particle diameter,  $d_p$  as given by Equation 3 but without any theoretical justification this modification would appear to be unsatisfactory. In addition, since there is considerable deviation from linearity in the curves in Fig. 13 it would seem that the theory of Lange does not explain the observed behaviour very well.

##### 4.2. Crack pinning theory of Evans

Several groups of workers have calculated from first principles the stresses required to propagate a crack through a matrix reinforced by an array of obstacles. This was done first of all by Evans [4] who used Lange's concepts that in a brittle particle reinforced composite, cracks can be impeded by obstacles in the form of second phase dispersions and that the primary cracks tend to bow out between the obstacles forming secondary

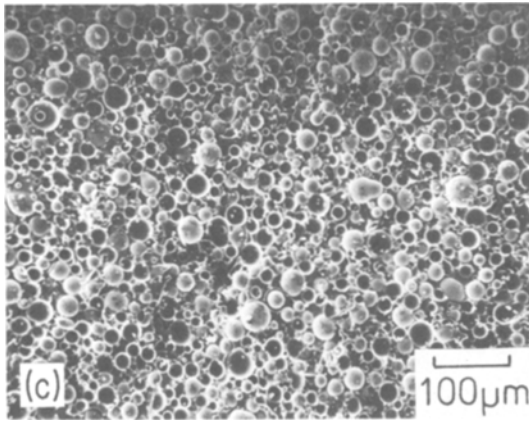
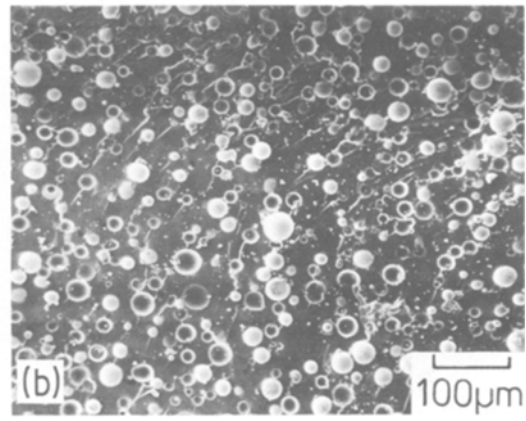
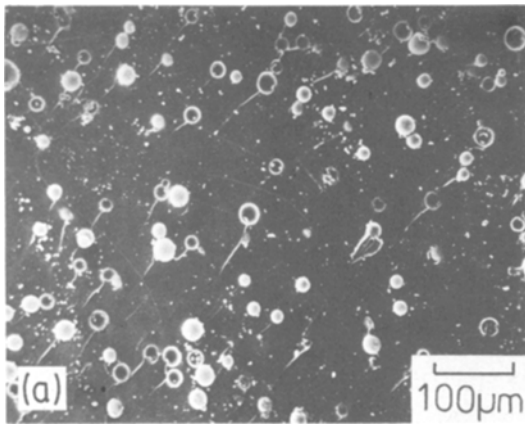


Figure 12 Scanning electron micrographs of the fracture surfaces of three different volume fractions of  $32\mu\text{m}$  diameter particles (cf. Figs. 5 and 10). (a)  $V_p = 0.10$ , (b)  $V_p = 0.30$ , and (c)  $V_p = 0.46$ .

cracks. He was thus able to determine the strength and increase in fracture energy of such a composite by calculating the stresses needed to propagate these secondary cracks. Details of the calculation can be obtained from the original publication [4] and only the final results are discussed here. These results are given in Table I where the ratio of the stress required to propagate a crack in the composite to the stress required for a crack in pure

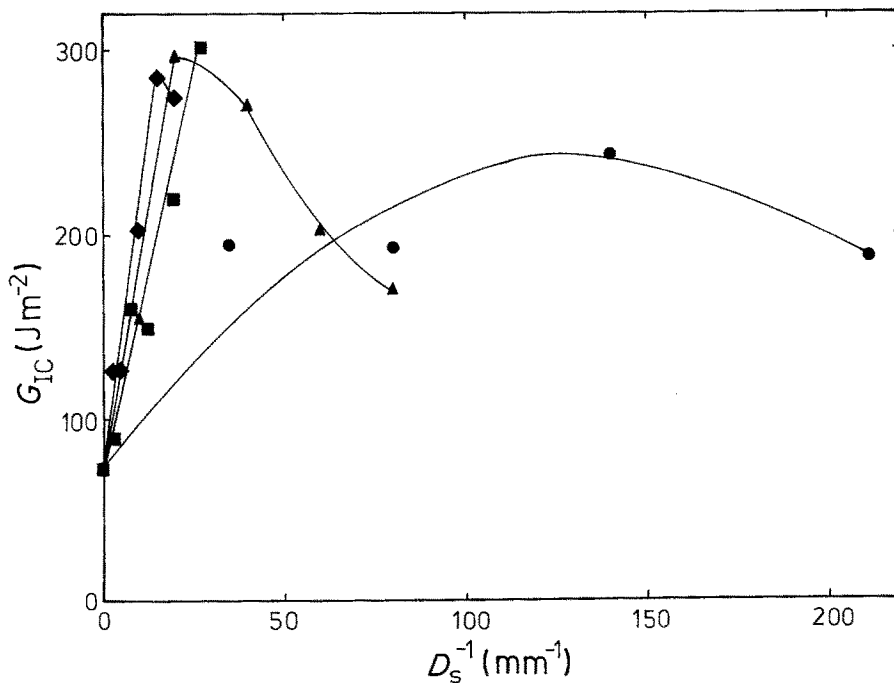


Figure 13 Dependence of  $G_{IC}$  (for crack initiation) upon the reciprocal of the interparticle separation,  $1/D_s$ . The symbols have the same meaning as in Fig. 8.

TABLE I Predicted values of  $\sigma_c/\sigma_0$  as a function of  $d_p/D_p$  for particle-filled composites

$d_p/D_p$	Non-interacting elliptical cracks		Interacting elliptical cracks	
	$\sigma_c/\sigma_0$ [12]	$\sigma_c/\sigma_0$ [4]	$\sigma_c/\sigma_0$ [12]	$\sigma_c/\sigma_0$ [4]
0	1	1	1	1
0.25	2.02	1.85	1.19	1.19
0.50	2.52	2.18	1.80	1.65
1.00	3.05	2.55	2.52	2.23
1.25	3.25	2.70	2.86	2.40
2.00	3.75	2.90	3.52	2.75

matrix,  $\sigma_c/\sigma_0$  is given in terms of the ratio of the particle diameter to the interparticle separation  $d_p/D_s$ . Values are given for both non-interacting and interacting elliptical secondary cracks.

Green *et al.* [11, 12] extended and modified Evans original analysis to account for penetrable obstacle shape and secondary crack interactions. In particular, they modified the analysis to take into account an accurate estimation of the exact position of the crack from when it breaks away from the pinning position. A similar variation of  $\sigma_c/\sigma_0$  with  $d_p/D_s$  was obtained by Green *et al.* [12] and their results are also given in Table I. It can be seen that somewhat higher values of  $\sigma_c/\sigma_0$  were obtained than by Evans for the corresponding value of  $d_p/D_s$ .

The problem arises as to how the results of these calculations can be used with the measured values of  $K_{Ic}$  or  $G_{Ic}$  as a function of  $V_p$ . In fact this can be done very easily since for a composite and an unfilled polymer sample containing cracks of the same length

$$\frac{\sigma_c}{\sigma_0} = \frac{K_{Ic}}{K_{Ic0}} = \left( \frac{E_c G_{Ic}}{E_0 G_{Ic0}} \right)^{1/2} \quad (8)$$

where  $K_{Ic}$  and  $K_{Ic0}$  are the critical stress intensity factor for the composite and matrix, respectively. Similarly  $E_c$  and  $E_0$ ,  $G_{Ic}$  and  $G_{Ic0}$  are the Young's moduli and fracture energies of the composite and polymer, respectively. The ratio  $d_p/D_s$  is a simple function of the particle volume fraction  $V_p$  since from Equation 2,

$$d_p/D_s = 3V_p/2(1 - V_p). \quad (9)$$

Hence the theories of crack pinning can be checked directly by comparing the measured variation of the ratio  $K_{Ic}/K_{Ic0}$  as a function of  $d_p/D_s$  with the theoretically calculated values.

### 4.3. Crack-tip blunting

It is now well established that in certain brittle polymers such as epoxy resins [16, 17] blunting at the crack tip can take place through localized shear yielding. This has the effect of causing crack propagation to become unstable (stick/slip) rather than continuous. In unfilled epoxy resins blunting can be induced by reducing the crosshead speed (or strain rate) or increasing the test temperature and a transition takes place from continuous to unstable propagation. This is due to the rate and temperature dependence of the yield stress [16, 17]. Although the temperature has not been varied in this present study, it has been found that for certain compositions stable propagation can be induced by increasing the crosshead speed (Figs. 3 and 4) – exactly as might be expected if blunting takes place – because the yield stress will increase as the crosshead speed is increased.

### 4.4. Analysis of propagation

It is clear that crack propagation in particle-filled epoxy resins is quite complex with both blunting and pinning taking place simultaneously. However, the situation can be simplified by removing the effect of blunting by extrapolating the data for initiation and arrest in Figs. 3 and 4 until the two lines meet. This occurs for most compositions at a crosshead speed of above about  $5 \text{ mm min}^{-1}$  unless propagation is already stable and blunting is not a problem. Once the effect of blunting is removed then the data can be compared with the theoretical predictions of Evans and others [4, 11, 12]. This is done in Fig. 14 where the measured values of  $K_{Ic}/K_{Ic0}$  for all volume fractions and particle sizes are plotted against  $d_p/D_s$  – the value of  $K_{Ic}$  being either the extrapolated value or the continuous value at about  $5 \text{ mm min}^{-1}$ . The solid lines represent the theoretically-calculated values determined by Green *et al.* [12]. It can be seen that agreement between the theory and experimental data is quite good. In contrast, if the effect of blunting is not removed the agreement is not so good and some of the experimental points lie well above the theoretical lines. It should be pointed out that the overall increase in  $K_{Ic}$  cannot be accounted for by blunting alone because  $K_{Ic}$  still increases with increasing  $d_p/D_s$  (or  $V_p$ ) when propagation is continuous. In order to increase  $K_{Ic}$  by blunting only, the addition of particles would have to reduce the yield stress of the material as in the case of rubber-modified

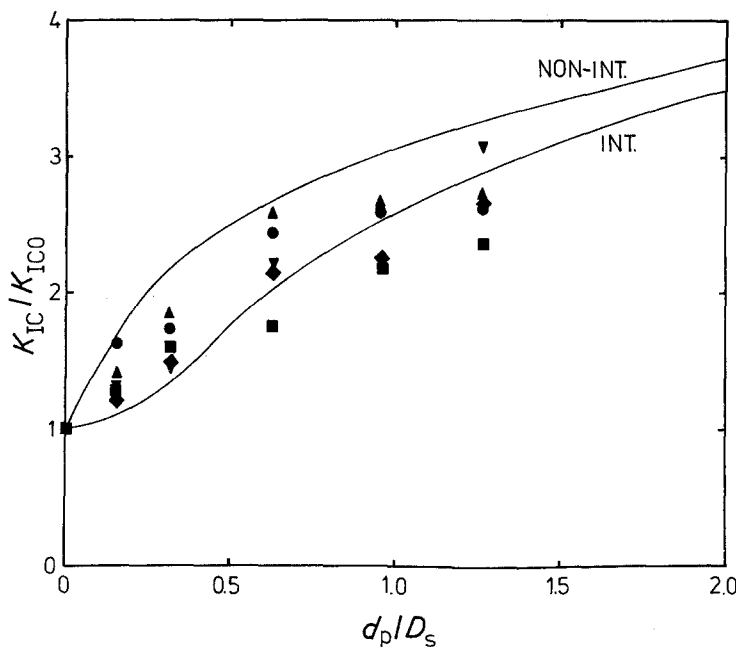


Figure 14 Variation of  $K_{IC}/K_{IC0}$  with  $d_p/D_p$  for the different composites. The lines represent the theoretical predictions of Green *et al.* [12] for interacting and non-interacting elliptical cracks. The symbols have the same meaning as in Fig. 8.

polymers [22] but it is well-established that the presence of glass particles increases the yield stress of brittle polymers [7].

Close examination of Fig. 14 shows that at higher values of  $d_p/D_s$  (or  $V_p$ ) some experimental points fall below the lower theoretical line. In addition it can be seen from Fig. 12 that as  $V_p$  increases there is a change in the fracture surface appearance. The tails which are associated with the pinning process are not seen in the composite with the highest volume fraction of particles. Close examination of the fracture surface in Fig. 12 shows that there has been considerable breakdown of the particle/matrix interface. This makes pinning more difficult and could explain why the measured values of  $K_{IC}/K_{IC0}$  are lower than predicted by the theory at high values of  $d_p/D_s$  (or  $V_p$ ). Breakdown of the particle/matrix interface will be affected by the strength of bonding between the particles and matrix and the presence of coupling or release agents [6]. The way in which the strength of this interface affects crack propagation will be the subject of Part II [21].

#### 4.5. Critical crack opening displacement criterion

There is strong evidence that crack propagation in many glassy polymers is controlled by a critical crack opening displacement criterion [1, 15]. It has been shown in particular that continuous crack propagation in epoxy resins is governed by

this criterion unless blunting occurs and causes unstable propagation [1, 15, 16]. It was demonstrated in the previous section that if the effects of blunting were removed then propagation in the glass-filled epoxy resins could be explained by pinning. It is therefore worth considering to what extent the fracture behaviour of the composites follows a critical crack opening displacement criterion when the effect of blunting is removed.

The critical crack-opening displacement criterion has been described in detail elsewhere [1, 15] and only the final results will be described here. The crack opening displacement,  $\delta$ , is

$$\delta = K_I^2 / \sigma_y E \quad (10)$$

which is given alternatively for a material which shows linear elastic behaviour as

$$\delta = \left( \frac{K_I}{E} \right)^2 \frac{1}{e_y} \quad (11)$$

where  $\sigma_y$  is the yield stress and  $e_y$  is the yield strain. If propagation occurs at a critical value of  $\delta$ ,  $\delta_c$  then it follows that

$$K_{IC} = E(\delta_c e_y)^{1/2}. \quad (12)$$

Normally  $e_y$  is approximately constant and so the criterion predicts that  $K_{IC}$  should be proportional to the Young's modulus,  $E$ .

In order to test the criterion for the particulate composites  $K_{IC}$  is plotted against  $E$  in Fig. 15a

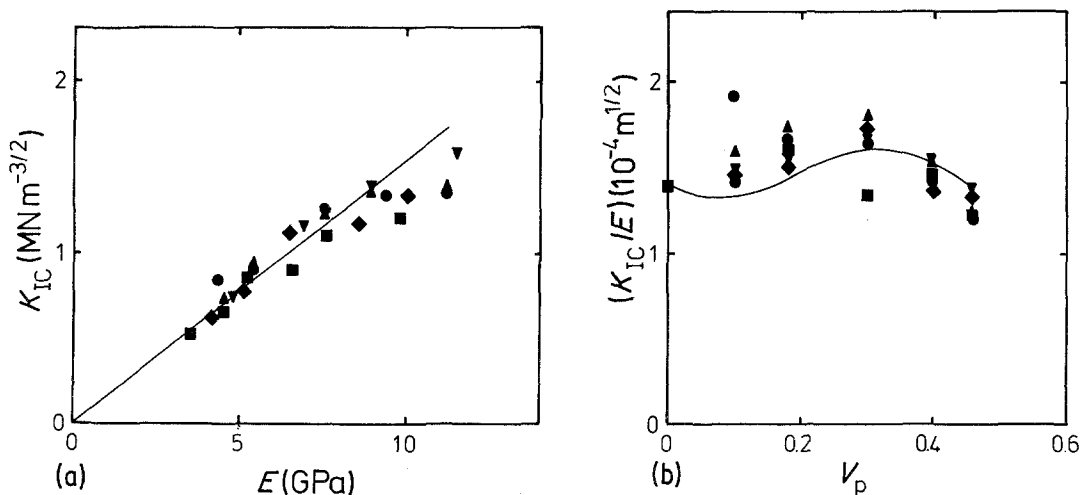


Figure 15 Critical crack-opening displacement criterion. (a) Variation of  $K_{IC}$  with  $E$  for all composite compositions. (b) Variation of  $K_{IC}/E$  with  $V_p$  for all composite compositions. The line is the theoretical prediction for pinning. (The symbols have the same meaning as in Fig. 8.)

for all of the composites studied – the values of  $K_{IC}$  being corrected for the effect of blunting by extrapolating the lines in Figs. 3 and 4 as in the previous section. The points lie close to a straight line through the origin which has a slope of  $1.54 \times 10^{-4} \text{m}^{1/2}$ . However, there is a tendency for the points to fall below the line at high values of  $K_{IC}$  and  $E$  (i.e. high volume fractions of particles). As explained in the previous section this could be due to breakdown of the particle/matrix interface or alternatively to a variation in  $e_y$  with  $V_p$ . However, it was found in a previous study that  $e_y$  did not vary with  $V_p$  for a particle-filled epoxy resin [8]. The yield strain,  $e_y$ , of the epoxy resin used in this present study was found to be about 0.06 [15] and so the value of  $\delta_c$  for the composite system used here is about  $0.4 \mu\text{m}$  and independent of particle size or volume fraction.

The question arises as to how the critical  $\delta_c$  criterion can be reconciled with the theories of crack pinning. The problem is similar to that of propagation in glassy thermoplastics where the mechanism of crack propagation is crazing but the criterion is a critical value of  $\delta_c$  [1]. Hence for the particle filled epoxy resin the principal mechanism of toughening is pinning whereas the criterion for crack growth is a critical  $\delta_c$  criterion. Since there are theoretical predictions for the variation of  $K_{IC}$  with  $V_p$  when pinning occurs [4, 12] and for the variation of  $E$  with  $V_p$ , it is possible to compare these predictions with the critical  $\delta_c$  criterion. This is done in Fig. 15b

where  $K_{IC}/E$  is plotted as a function of  $V_p$ . The solid line is the theoretical determined from the calculation of  $K_{IC}$  for crack pinning by Green *et al.* [12] and from the values of  $E$  determined using Equation 6. The experimental values of  $K_{IC}/E$  for all the composites are also plotted. It can be seen that the points fall close to the theoretical line and the line is approximately horizontal – exactly as required by the critical  $\delta_c$  criterion (Equation 12). Hence it can be concluded that when pinning occurs both the theoretical predictions and experimental measurements of crack propagation are consistent with a critical crack opening displacement criterion.

#### 4.6. Variation of $G_{IC}$ with $V_p$

Many previous investigations of the fracture of particle-filled polymers have concentrated upon the dependence of the fracture energy of  $G_{IC}$  upon  $V_p$  [6, 7, 9, 10, 13]. A great deal of significance has been placed upon peaks in  $G_{IC}$  which occur at particular values of  $V_p$  (cf. Fig. 10) and they have been explained in terms of a change in failure mechanism [13]. This present study has concentrated upon the variation of the critical stress intensity factor  $K_{IC}$  rather than  $G_{IC}$  with structure and has enabled the principal failure mechanisms, pinning and blunting to be identified. Concentrating only upon  $G_{IC}$  in this context can be misleading. For example, the theory of pinning predicts that a plot of  $G_{IC}$  against  $V_p$  should peak even when pinning is the only toughening mechanism. This can be seen in Fig. 16 where  $G_{IC}/G_{IC0}$

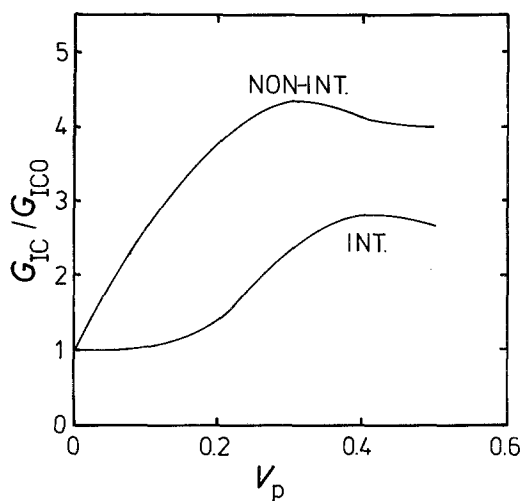


Figure 16 Variation of  $G_{IC}/G_{IC0}$  with  $V_p$ . The lines are the theoretical predictions of Green *et al.* [12] for interacting and non-interacting elliptical cracks.

is plotted against  $V_p$ . The values of  $G_{IC}$  were obtained from Equation 5 using the values of  $K_{IC}$  predicted by the theory of Green *et al.* [12] and  $E$  determined using Equation 6. It can be seen that there are peaks for both interacting and non-interacting secondary cracks. The peaks take place between volume fractions between 0.3 and 0.4 which is similar to the position of the peaks observed in practice [6, 7, 13]. Hence the peaks can occur without an associated change in failure mechanism. Clearly,  $G_{IC}/G_{IC0}$  could be further modified by blunting especially if no blunting occurs in the unfilled matrix. The exact dependence of  $G_{IC}$  upon  $V_p$  will depend upon the relative contributions of pinning and blunting.

## 5. Conclusions

A detailed study has been made of the effect of particulate reinforcement upon crack propagation in a glass particle-filled epoxy resin system. The following observations have been made:

(i) The mechanism of toughening is crack-front pinning.

(ii) When pinning takes place a critical crack opening displacement criterion can be applied.

(iii) Further toughening can take place through crack blunting but the effectiveness of pinning may be reduced by breakdown of the particle/matrix interface.

(iv) Peaks in plots of  $G_{IC}$  against particle volume fraction can occur when pinning is the only fracture mechanism. They do not necessarily indicate a change in mechanism.

## Acknowledgements

This project was supported in part by an SERC Research Grant. The authors are also grateful to Dr A. J. Kinloch for useful discussion.

## References

1. A. J. KINLOCH and R. J. YOUNG, "Fracture Behaviour of Polymers" (Applied Science, London, 1983), Chap. 11.
2. C. B. BUCKNALL, *Adv. Polym. Sci.* **27** (1978) 121.
3. F. F. LANGE, *Phil. Mag.* **22** (1970) 983.
4. A. G. EVANS, *ibid.* **26** (1972) 1327.
5. A. C. MOLONEY, H. H. KAUSCH and H. R. STEIGER, *J. Mater. Sci.* **18** (1983) 208.
6. L. J. BROUTMAN and S. SAHU, *Mater. Sci. Eng.* **8** (1971) 98.
7. P. K. MALLICK and L. J. BROUTMAN, *ibid.* **18** (1975) 63.
8. R. J. YOUNG and P. W. R. BEAUMONT, *J. Mater. Sci.* **12** (1977) 684.
9. F. F. LANGE and K. C. RADFORD, *ibid.* **6** (1971) 1197.
10. K. C. RADFORD, *ibid.* **6** (1971) 1286.
11. D. J. GREEN, P. S. NICHOLSON and J. D. EMBURY, *ibid.* **14** (1979) 1413.
12. *Idem*, *ibid.* **14** (1979) 1657.
13. S. K. BROWN, *Brit. Polym. J.* (1980) 24.
14. F. F. LANGE, *J. Amer. Chem. Soc.* **54** (1971) 614.
15. R. A. GLEDHILL, A. J. KINLOCH, S. YAMINI and R. J. YOUNG, *Polymer* **19** (1978) 574.
16. S. YAMINI and R. J. YOUNG, *J. Mater. Sci.* **15** (1980) 1823.
17. A. J. KINLOCH and J. G. WILLIAMS, *ibid.* **15** (1980) 987.
18. J. SPANOUDAKIS, "Fracture in Particle-Filled Epoxy Resins", PhD thesis, University of London, (1981).
19. O. ISHAI and L. J. COHEN, *Int. J. Mech. Sci.* **9** (1967) 539.
20. A. G. LEWIS and L. E. NEILSEN, *J. Appl. Polym. Sci.* **14** (1970) 1449.
21. J. SPANOUDAKIS and R. J. YOUNG, *J. Mater. Sci.* **19** (1984) 000.
22. A. J. KINLOCH, S. J. SHAW and D. L. HUNSTON, to be published.

Received 10 May  
and accepted 26 May 1983